Physics Letters B 804 (2020) 135396

Contents lists available at ScienceDirect

Physics Letters B

www.elsevier.com/locate/physletb

Observation of strong reduction of multiple scattering for channeled particles in bent crystals

W. Scandale [a], G. Arduini [a], F. Cerutti [a], M. Garattini [a,j], S. Gilardoni [a], R. Losito [a], A. Masi [a], D. Mirarchi [a], S. Montesano [a], S. Redaelli [a], R. Rossi [a,e], G. Smirnov [a], D. Breton [b], L. Burmistrov [b], V. Chaumat [b], S. Dubos [b], J. Maalmi [b], V. Puill [b], A. Stocchi [b], E. Bagli [c], L. Bandiera [c], M. Romagnoni [c], V. Guidi [c], A. Mazzolari [c], F. Murtas [a,d], F. Addesa [a,e], G. Cavoto [e,k], F. Iacoangeli [e], F. Galluccio [f], A.G. Afonin [g], Yu.A. Chesnokov [g], A.A. Durum [g], V.A. Maisheev [g], Yu.E. Sandomirskiy [g], A.A. Yanovich [g], A.D. Kovalenko [h], A.M. Taratin [h,*], A.S. Denisov [i], Yu.A. Gavrikov [i], Yu.M. Ivanov [i], L.P. Lapina [i], L.G. Malyarenko [i], V.V. Skorobogatov [i], G. Auzinger [j], J. Borg [j], T. James [j], G. Hall [j], M. Pesaresi [j]

[a] CERN, European Organization for Nuclear Research, CH-1211 Geneva 23, Switzerland
[b] Laboratoire de l'Accelerateur Lineaire (LAL), Universite Paris Sud Orsay, Orsay, France
[c] INFN Sezione di Ferrara and Dipartimento di Fisica e Scienze della Terra, Università di Ferrara, Via Saragat 1 Blocco C, 44121 Ferrara, Italy
[d] INFN LNF, Via E. Fermi, 40, 00044 Frascati (Roma), Italy
[e] INFN Sezione di Roma, Piazzale Aldo Moro 2, 00185 Rome, Italy
[f] INFN Sezione di Napoli, Italy
[g] Institute for High Energy Physics in National Research Centre "Kurchatov Institute", 142281, Protvino, Russia
[h] Joint Institute for Nuclear Research, Joliot-Curie 6, 141980, Dubna, Russia
[i] Petersburg Nuclear Physics Institute in National Research Centre "Kurchatov Institute", 188300, Gatchina, Russia
[j] Blackett Laboratory, Imperial College, London SW7 2AZ, UK
[k] Dipartimento di Fisica, Sapienza Università di Roma, Piazzale A. Moro, 2, 00185 Roma, Italy

ARTICLE INFO

Article history:
Received 24 January 2020
Received in revised form 3 March 2020
Accepted 21 March 2020
Available online 26 March 2020
Editor: L. Rolandi

Keywords:
Crystal
Channeling
Multiple scattering
Dechanneling
Beam deflection

ABSTRACT

Strong reduction of multiple scattering for channeled particles has been observed in an experiment on the deflection of a 180 GeV/c π^+-meson beam by bent silicon crystals. The RMS deflections due to multiple scattering for the channeled particles were about six times smaller than for non-channeled ones. It was shown that the approach suggested recently for the description of multiple scattering for channeled particles using the experimental data for random crystal orientations gives fair agreement with the experiment.

1. Introduction

When high energy charged particles enter a crystal with small angles relative to the crystal planes, $\theta_0 \ll 1$, their transverse motion is governed by a crystal potential, $U(x)$, averaged along the planes [1]. If the angles are smaller than the critical angle $\theta_o < \theta_c = (2U_o/pv)^{1/2}$, where p, v are the particle momentum and velocity, respectively, and U_o is the well depth of the averaged planar potential, the particles can be captured into the channeling regime. Channeled particles move in a crystal oscillating between two neighboring planes. Channeling is also possible in a bent crystal if its bend radius is larger than the critical value, $R > R_c = pv/eE_m$ [2], where E_m is the maximum strength of the electric field in the planar channel.

Incoherent (multiple and single) scattering in close collisions with atomic nuclei and electrons of the crystal changes the trans-

* Corresponding author.
E-mail address: alexander.taratin@cern.ch (A.M. Taratin).

https://doi.org/10.1016/j.physletb.2020.135396

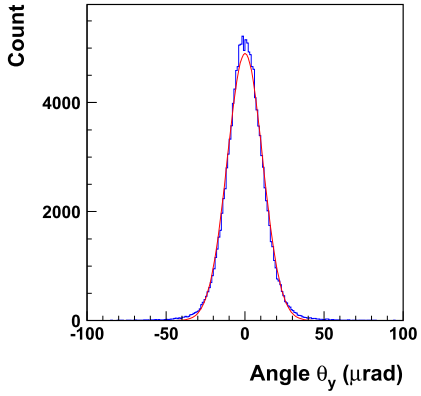

Fig. 1. The distribution of vertical deflection angles of 180 GeV/c π^+-mesons for the background conditions without a crystal. The curve is a Gaussian fit of the distribution.

verse energy of channeled particles, and they may leave the channeling regime (the process of dechanneling).

In the case of planar orientations far from the main axes the deflection angle distribution of particles in the direction parallel to the crystal planes is determined only by incoherent scattering. Therefore, these distributions can be used to study multiple scattering for channeled particles. The variance of the distribution due to multiple scattering in the crystal may be found as

$$\sigma^2 = \sigma_{ex}^2 - \sigma_{bg}^2, \tag{1}$$

where σ_{ex} and σ_{bg} are the RMS deflections measured with and without a crystal in the particle beam. The density of atomic nuclei and electrons averaged along the trajectories of channeled particles with small oscillation amplitudes is smaller than for the amorphous crystal orientations when only incoherent scattering of incident particles occurs in a crystal. Therefore, a reduction of multiple scattering for the channeled fraction has been observed in [3].

This paper presents the measurement results for multiple scattering of a 180 GeV/c π^+-meson beam in two bent silicon crystals with length of 23 mm and 4 mm for their optimal orientations for channeling. The critical angle in this case for the (110) planes $\theta_c \approx 16$ μrad. We consider the Gaussian approximation of the projected angular distributions of pion multiple scattering in the vertical plane which is orthogonal to the channeling one. Strong reduction of multiple scattering has been observed for the channeled fraction of the pion beam. The experimental results are compared with simulations using the model described in [4].

2. Experimental layout and results

The experimental setup at the H8 beamline of the CERN SPS was the same as described in [5]. Five pairs of silicon microstrip detectors D_1-D_5, two upstream and three downstream of the crystal, were used to measure both incoming and outgoing angles of the particles. The distances of about 10 m and 11 m were between the two first and the two last detectors, respectively. The detector spatial resolution was measured to be about 7 μm. The beam angular divergence in the horizontal and vertical directions were $\sigma_x = (29 \pm 0.03)$ μrad and $\sigma_y = (35.9 \pm 0.04)$ μrad, respectively.

The difference of the outgoing and incoming angles gives the deflection angle for each particle. Fig. 1 shows the distribution of vertical deflection angles for background conditions without a crystal. The histogram was fitted by a Gaussian giving the RMS deflection $\sigma_{\text{bg}} = (11.27 \pm 0.01)$ μrad, which determines the resolution of deflection angles.

The crystals with the largest faces parallel to the (110) crystallographic planes were fabricated at INFN-Ferrara according to the

Table 1
Crystal parameters.

Parameter	Crystal 1	Crystal 2
Length (mm)	23	4
Bend angle (μrad)	1067 ± 1	62 ± 1
Bend radius (m)	21.56 ± 0.02	64.5 ± 1.0

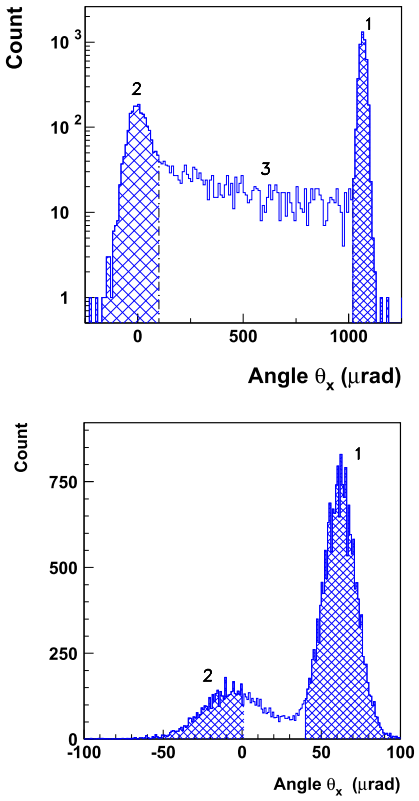

Fig. 2. The distribution of horizontal deflection angles of particles for the optimal orientations of crystal 1 (a) and 2 (b) for channeling. Peak 1 consists of the channeled particles. Peak 2 is formed by non-channeled particles, which were not captured into the channeling regime. Particles in range 3 were dechanneled during the passage through the crystal.

methodology described in [6,7]. The crystal parameters are given in Table 1. The crystal radii are large in comparison with the critical one, $R_c = 0.3$ m for the considered particle energy. Therefore, the effective potentials are close to the straight crystal potential. So, the channeling conditions are practically identical in both crystals. The different results of the beam deflection are obtained because of the different lengths and bend angles of the crystals.

The crystal under study was placed vertically and bent along its height. The induced anticlastic curvature along the crystal length was used to deflect particles in the horizontal plane. A high precision goniometer was used to align the (110) crystal planes with respect to the beam direction with an accuracy of 2 μrad. The accuracy of preliminary crystal alignment using a laser beam was about 0.1 mrad. An angular scan was performed and the optimal orientation was found which gives the maximum of the deflected beam fraction.

Fig. 2a shows the distribution of horizontal deflection angles for the optimal orientation of long crystal 1. A narrow fraction of the beam corresponding to those particles contained in an incoming angular range ±1.25 μrad was considered. The angular resolution of incoming angles was estimated to be about 5.8 μrad. Particle trajectories in the horizontal plane are determined by the averaged potential of the bent planes in the first approximation. Peak 1 on the right consists of the particles which passed through

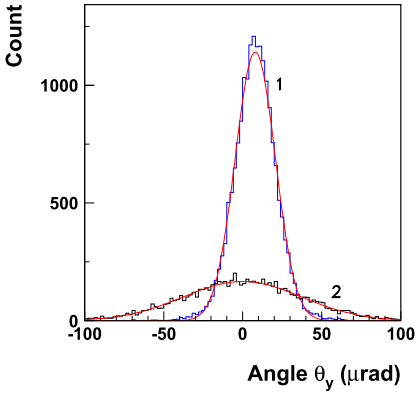

Fig. 3. The vertical deflection angle distributions for the channeled (1) and non-channeled (2) beam fractions shown in Fig. 2a. The curves are Gaussian fits of the distributions.

Table 2
RMS deflections due to multiple scattering for channeled and non-channeled fractions.

Parameter	σ_{ch} (μrad)	σ_{nch} (μrad)	σ_{nch}/σ_{ch}
Crystal 1	5.88 ± 0.17	35.64 ± 0.38	6.06
Crystal 2	2.56 ± 0.32	14.61 ± 0.30	5.71

Table 3
Multiple scattering parameters for channeled (CH) and non-channeled (NCH) fractions.

Parameter	$d\sigma^2/dz$ (μrad^2/mm) CH	CH/AM	$d\sigma^2/dz$ (μrad^2/mm) NCH	NCH/AM
Crystal 1	1.50 ± 0.09	0.031	55.23 ± 1.18	1.134
Crystal 2	1.64 ± 0.41	0.034	53.35 ± 2.19	1.096

the whole crystal in the channeling regime. The maximum of the peak is at an angle $\theta_{ch} = 1067$ μrad and its position corresponds to the crystal bend angle $\alpha = \theta_{ch}$. The number of particles in peak 1 determines the deflection (channeling) efficiency, which is $P_d = (54.3 \pm 0.8)\%$. Peak 2 on the left is formed by those particles which were not captured into the channeling regime. Particles in range 3 with deflection angles between two maxima are the dechanneled ones. They are seen clearly in the logarithmic scale used for this purpose in the figure.

Vertical deflection angles of particles in the crystal are determined only by multiple scattering in close collisions with the atomic nuclei and electrons. Fig. 3 shows the vertical deflection angle distributions for the channeled 1 and non-channeled 2 beam fractions. The distribution for the channeled fraction is about three times narrower than for the non-channeled one. Both histograms were fitted by a Gaussian giving the RMS deflections $\sigma_{ex1} = (12.71 \pm 0.08)$ μrad and $\sigma_{ex2} = (37.38 \pm 0.36)$ μrad, respectively. Then the variance of the particle deflection distributions due to multiple scattering in the crystal were found for the channeled and non-channeled fractions as

$$\sigma_{ch}^2 = \sigma_{ex1}^2 - \sigma_{bg}^2, \qquad \sigma_{nch}^2 = \sigma_{ex2}^2 - \sigma_{bg}^2.$$

Table 2 shows the corresponding RMS deflections due to multiple scattering in the crystal. The RMS deflection value for the channeled fraction is about six times smaller than for the non-channeled one. Table 3 shows the average rate of the increase of variance for multiple scattering of particles in the crystal and its ratio to the value for the amorphous crystal orientation (AM). The last one was measured for 400 GeV/c protons in [8] and was recalculated for 180 GeV/c π^+-mesons (see below). The variance increase rate for the channeled fraction is only about 3% of the amorphous orientation case.

The measurements for crystal 2 were similar. Fig. 2b shows the horizontal deflection angle distribution for the optimal orientation of the crystal 2 for channeling. The same narrow beam fraction with an incoming angular range ±1.25 μrad was considered. The deflection efficiency is higher, about 71.7%, due to the smaller dechanneled fraction for this shorter crystal. The channeled 1 and non-channeled 2 fractions are shown by the hatched histogram parts. Parameters of multiple scattering distributions obtained for crystal 2 are shown in Table 2 and 3. The RMS deflection due to multiple scattering in the crystal for the channeled fraction is also about six times smaller than for the non-channeled one. It should be noted that the variance increase rate for the channeled fraction in this short crystal is higher than for long crystal 1, about 3.4% of the amorphous orientation value, see Table 3.

The variance increase rate for the non-channeled fractions considered are larger than for the AM case because the atomic density averaged along the particle trajectories in the volume reflection area near the crystal entrance is higher than the average one [9].

3. Simulations of multiple scattering

Multiple scattering of channeled particles in close collisions with atomic nuclei (n) and electrons (e) in the crystal depends on the particle position in the planar channel, and for the mean square of the deflection angle projection per unit length is written as follows [10]

$$\overline{\frac{d\theta_x^2}{dz}}_n(x) = \overline{\frac{d\theta_x^2}{dz}}_{nR} \cdot P_n(x), \qquad \overline{\frac{d\theta_x^2}{dz}}_e(x) = \overline{\frac{d\theta_x^2}{dz}}_{eR} \cdot \frac{\rho(x)}{NZ}, \tag{2}$$

where $\overline{d\theta_x^2/dz}_R$ are the corresponding values for a random (amorphous) crystal orientation, $P_n(x)$ is the transverse distribution of the crystal plane atoms due to thermal vibrations, which was considered as a normal one with the RMS vibration amplitude $u_1 = 0.075$ Å, N is the atomic density, Z is the atomic number, NZ is the average electron density, $\rho(x)$ is the electron density in a planar channel. The latter was calculated taking into account thermal vibrations of the crystal atoms and the contribution of the two neighboring planes using the Moliere approximation for the atomic potential [4]. The contribution from the scattering on nuclei is much larger near the edge of the channel, whereas the contribution from the scattering on electrons is considerably larger in the middle of the channel.

The mean square deflection (MSD) value for 400 GeV/c protons in silicon crystals for their amorphous orientations $\overline{d\theta_x^2/dz}_R$ has been recently measured in [8]. The corresponding value for 180 GeV/c particles can be found using the proportionality, $\overline{d\theta_x^2/dz}_R \sim 1/p^2$, $\overline{d\theta_x^2/dz}_R = 48.69$ μrad^2/mm. The partial contributions due to the scattering on atomic electrons and nuclei can be found from the MSD experimental value according to [11] as follows

$$\overline{\frac{d\theta_x^2}{dz}}_{eR} = \overline{\frac{d\theta_x^2}{dz}}_R \cdot \frac{1}{Z+1}, \qquad \overline{\frac{d\theta_x^2}{dz}}_{nR} = \overline{\frac{d\theta_x^2}{dz}}_R \cdot \frac{Z}{Z+1}. \tag{3}$$

This approach (2), (3) for the calculation of multiple scattering in the oriented crystals has been recently used for the simulation of 180 GeV/c particles dechanneling in a 23 mm long bent silicon crystal [12]. Fair agreement of these simulations with the experiment has been observed.

Simulations of multiple scattering of a 180 GeV/c π^+-meson beam by the bent crystals 1 and 2 for the experimental conditions described above have been made using the model [4]. The particle

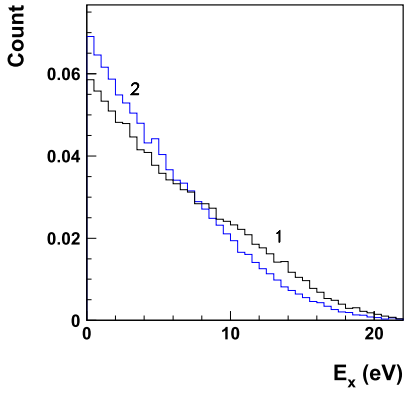

Fig. 4. The particle distributions in the transverse energy E_x obtained by simulations for two different depths of 4 mm (1) and 23 mm (2) in crystal 1.

trajectories were calculated by numerically solving the equation of motion in the effective potential of the crystal bent planes. The change of the transverse velocity of a particle due to multiple scattering on the atomic electrons and nuclei was calculated using the experimental values from (2) and (3) at each step along the particle trajectory. The step length was much smaller than the spatial period of the particle oscillations in the channel. The RMS deflections due to multiple scattering for the channeled fractions σ_{ch} were found to be (5.57 ± 0.02) μrad and (2.53 ± 0.01) μrad for the crystal 1 and 2, respectively. The RMS values obtained by simulations are close to the experimental ones shown in Table 2.

Fig. 4 shows the particle distributions in the transverse energy E_x for two different depths of 4 mm (1) and 23 mm (2) in crystal 1. The distribution evolution along the crystal length due to multiple scattering reduces the fraction of particles with large oscillation amplitudes. The evolution should reduce the mean square deflection due to multiple scattering for larger depths in a crystal. This is a possible explanation of the larger value of the mean rate of the variance increase due to multiple scattering observed for short crystal 2 in comparison with crystal 1 (Table 3).

4. Conclusions

The experiment has shown a strong reduction of pion multiple scattering for the channeled beam fractions. The RMS deflections for these fractions were about six times smaller than for the non-channeled fractions. It was shown that the approach suggested recently [12] for the description of multiple scattering for channeled particles using the experimental data [8] for amorphous crystal orientations gives fair agreement with the experimental results.

Declaration of competing interest

The authors declare that they have no known competing financial interests or personal relationships that could have appeared to influence the work reported in this paper.

Acknowledgements

The Imperial College group thanks the UK Science and Technology Facilities Council for financial support. The INFN authors acknowledge the support of the ERC Ideas Consolidator Grant No. 615089 CRYSBEAM. The IHEP participants of UA9 experiment acknowledge financial support of Russian Science Foundation (grant 17-12-01532).

References

[1] J. Lindhard, K. Dan, Vidensk. Selsk. Mat. Fys. Medd. 34 (14) (1965).
[2] E.N. Tsyganov, Preprint TM-682, TM-684, Fermilab, Batavia, 1976.
[3] W. Scandale, et al., Eur. Phys. J. C 79 (2019) 993.
[4] A.M. Taratin, S.A. Vorobiev, Sov. Phys. Tech. Phys. 30 (1985) 927.
[5] M. Pesaresi, et al., J. Instrum. 6 (2011) P04006;
G. Hall, G. Auzinger, J. Borg, T. James, M. Pesaresi, M. Raymond, Nucl. Instrum. Methods A 924 (2019) 394.
[6] S. Baricordi, et al., Appl. Phys. Lett. 91 (2007) 061908.
[7] S. Baricordi, et al., J. Phys. D, Appl. Phys. 41 (2008) 245501.
[8] W. Scandale, et al., Nucl. Instrum. Methods B 402 (2017) 291.
[9] W. Scandale, A.M. Taratin, Phys. Rep. 815 (2019) 1.
[10] M. Kitagava, Y.H. Ohtsuki, Phys. Rev. B 8 (1973) 3117.
[11] H.A. Bethe, Phys. Rev. 89 (1953) 1256.
[12] W. Scandale, et al., Nucl. Instrum. Methods B 438 (2019) 38.